Journal of Applied Polymer Science

Electrical Insulation Characteristics of Alumina, Titania, and Organoclay Nanoparticles Filled PP/EPDM Nanocomposites

Muhammad Safwan Hamzah,[1] Mariatti Jaafar,[1] Mohamad Kamarol Mohd Jamil[2]

[1]School of Materials and Mineral Resources Engineering, Engineering Campus, Universiti Sains Malaysia, Nibong Tebal, Pulau Pinang 14300, Malaysia

[2]School of Electrical and Electronic Engineering, Engineering Campus, Universiti Sains Malaysia, Nibong Tebal, Pulau Pinang 14300, Malaysia

Correspondence to: M. Jaafar (E-mail: mariatti@usm.my)

ABSTRACT: In this study, nanofillers composed of alumina, titania, and organoclay were separately embedded in 50% polypropylene (PP) and 50% ethylene propylene diene monomer (EPDM) blends. Several formulations of PP/EPDM nanocomposites were prepared using an internal mixer and were molded using a compression mold to produce test samples. The effects of filler loading (2, 4, 6, and 8 vol %) on the dielectric breakdown strength, dielectric properties, hydrophobicity, and flammability were determined. The addition of nanofillers improved the breakdown strength (up to 2 vol %) and increased the dielectric constant and dielectric loss of the PP/EPDM nanocomposites. The hydrophobicity of PP/EPDM/Al_2O_3 increased, whereas the hydrophilicity of PP/EPDM/TiO_2 and PP/EPDM/organoclay increased. Flammability test results showed that PP/EPDM/TiO_2 had a lower burning rate than PP/EPDM/Al_2O_3 and PP/EPDM/organoclay. © 2014 Wiley Periodicals, Inc. J. Appl. Polym. Sci. **2014**, *131*, 41184.

KEYWORDS: applications; dielectric properties; elastomers; nanoparticles; nanowires and nanocrystals; thermoplastics

Received 23 September 2013; accepted 15 June 2014
DOI: 10.1002/app.41184

INTRODUCTION

In the early development of polymeric insulators, neat polymer was used, and its insulation properties are enhanced by the addition of micron fillers. However, the enhancement is minimal and the breakdown strength of the insulators may be reduced.[1] Polymer nanocomposites are promising materials that can be used to enhance the engineering macroscopic properties of polymeric insulators. Polymer nanocomposites are composite materials that contain inorganic particles of nanosized dimensions that are homogeneously dispersed into the polymer matrix. This new type of polymeric insulators has gained increasing attention over the past few years because nanocomposite or nanostructured polymers can improve the electrical, mechanical, and thermal properties of the bulk material as compared with neat polymers.[2] During outdoor service, the surface of the insulating materials is frequently subjected to moisture and contamination, which leads to reduction in electrical insulation. Compared with traditional glass or ceramic insulation systems, polymer nanocomposite insulators have several advantages, which include low surface energy. Low surface energy is related to a surface that is not easily wet or exhibit high contact angle and it remain hydrophobic in a wet condition, such as when the material is exposed to fog, dew, or rain.[3] The use of polymer nanocomposites as insulators is expected to increase significantly in the future because fabrication costs are reduced and these materials have considerable advantages such as high mechanical strength to weight ratio, resistance to vandalism, and good performance despite the presence of heavy pollution and in wet conditions.[4] Flammability is also one of the requirements to be used as an insulator. Better dispersion of nanofillers will result in better stability of the polymer and decrease in polymer flammability.

The use of polymer insulation, such as ethylene propylene diene monomer (EPDM) has been reported in previous works.[4] EPDM is used in electrical insulation because of its combination of superior electrical properties, flexiblility over a wide temperature range, and resistance to moisture and weather.[4] However, synthetically produced EPDM is relatively expensive as compared with other conventional elastomers.[5] Polypropylene (PP) as a high-volume commodity plastic has very interesting characteristics, such as low density, good surface hardness, and excellent price performance ratio.[6] PP is blended with EPDM in order to reduce the production cost and toughened the blend system. For several decades, the use of PP/EPDM blends has been continuously growing in various industrial domains. PP/EPDM blends offer a wide spectrum of materials from elastified

PP to EPDM rubber reinforced with thermoplastic because PP mixing in any ratio is possible.[6,7]

Addition of talc in a PP/EPDM system has been reported by Öksüz et al.,[8] it is found that the use of annealing heat treatment increased its tensile strength, yield strength, elastic modulus, and impact strength. Previous studies on PP/EPDM focused more on their mechanical properties,[7,8] rheology,[9] and morphology.[10] However, the effect of PP/EPDM on electrical insulation characteristics has not been adequately studied yet. In the present study, three types of nanofillers, namely, aluminum oxide (Al_2O_3), titanium dioxide (TiO_2), and organoclay, were added to the PP/EPDM formulation. The dielectric breakdown strength, dielectric properties, hydrophobicity, and flammability of the nanocomposites of nanofiller-filled PP/EPDM were evaluated.

EXPERIMENTAL

Materials

The homopolymer PP (Titanpro 6431) was a commercial product from Titan Polymer (M) Sdn. Bhd. with a melt index of 7 g/10 min and a density of 0.9 g/cm^3. EPDM-grade Buna EP G 2070 (Mooney viscosity, 25 ± 5 MU; density, 0.86 g/cm^3) containing 73 wt % ethylene was supplied by LANXESS Deutschland GmbH. Aluminum oxide (Al_2O_3) and titanium dioxide (TiO_2) were supplied by Sigma-Aldrich (M) Sdn. Bhd. Organoclay type Cloisite 15A (in a layered structure form) is a natural montmorillonite modified with a dimethyl dehydrogenated tallow quarternary ammonium having a cation exchange capacity of 125 mequiv/100 g[11–13] was used in the study. Al_2O_3 and TiO_2 were used as received without any surface modification. The particle sizes of Al_2O_3, and TiO_2 are 12 and 25 nm, respectively. The organoclay with a thickness of 1 and 40 nm diameter were supplied by Southern Clay Products, Dicumyl peroxide (DCP) was obtained from Bayer (M) Sdn. Bhd. All materials were commercially available and used without further purification.

Composite Preparation

The PP/EPDM blends were prepared by mixing the polymer and the filler powders in an internal mixer followed by compression molding. The temperature and the rotor speed of the internal mixer were set to 180°C and 50 rpm, respectively. The ratio of PP/EPDM was fixed at 50/50, and the blending sequence was initiated using PP, EPDM, nanofillers, and DCP for 10 min. After the compounding process, the filled PP/EPDM nanocomposites were compression-molded to form a plate with thicknesses of 1 and 3 mm in an electrically heated hydraulic press at 185°C. The samples were preheated for 6 min and held at a pressure of 1500 psi for 2 min. Cooling was then carried out at the same pressure for 3 min.

Characterization

The fracture surface morphology of the selected PP/EPDM composites was characterized using a field emission-scanning electron microscope (FE-SEM; model ZEISS SUPRA 35 VP). The fracture surface of the sample was coated with a gold-palladium layer by using a Sputter Coater Polaron SC 515 to avoid electrostatic charging during observation. The dielectric breakdown strength was measured based on IEC60243-1 standard. The stainless steel plane-plane electrodes with a diameter of 25 mm were used in this experiment. Each sample with the thickness of 1 ± 0.1 mm was placed between the two electrodes, and an incremental AC voltage rate of 500 V/s was applied until electrical breakdown occurs. The samples and electrodes were immersed in transformer oil to prevent flashover. The dielectric breakdown strength (kV/mm) was determined by dividing the breakdown voltage (kV) with the thickness (mm) of the samples. Ten samples for each composition were tested and the results were analyzed using Weibull statistical analysis. The dielectric constant and dielectric loss of the PP/EPDM composites were measured using a Hewlett Packard 4291B LCR Meter. For dielectric measurements, disk-like shape specimens of 1 cm diameter were cut from the prepared sheets. The test specimen is placed firmly between two copper electrodes connected through cables to the impedence analyzer. The measurements were performed in the frequency range of 1 MHz to 1 GHz at room temperature. The equations used in calculating the dielectric properties are based on previous works.[14,15] The surface hydrophobicity was classified by determining the contact angle by the sessile drop technique. A droplet of a purified liquid (distilled water) was placed on the sample surface by using a syringe. The resulting angle between the droplets was measured using a goniometer or a charge coupled camera device (CCD) fitted onto a microscope. Five measurements on different parts of the samples were averaged. All tests were carried out at room temperature. The rate of burning was subjected to a flammability test based on the ASTM D 635 method. The nanocomposite sheet was cut into bar-shaped test specimens with a dimension of 125 × 13 × 3 mm^3. At least ten specimens were prepared for each composition and composite system. The gauge length was fixed to 25 mm, and the average rate of burning was reported in millimeters per minute. All tests were performed at room temperature.

RESULTS AND DISCUSSION

Dielectric Breakdown Strength

The dielectric breakdown strength was investigated to determine the maximum voltage that can be applied to the materials before dielectric failure occurs. The dielectric breakdown test of polymers usually involve multiple samples because of statistical variations in the recorded values of breakdown strength. A study has reported that even though the samples are identical, the extent of breakdown strength of the specimens may be significantly different.[16] The dielectric breakdown data are known to be in good agreement with the Weibull distribution, which can be expressed by eq. (1).[17,18]

$$F(Et) = 1 - \exp\left[-\left(\frac{Et}{Et_s}\right)^{\beta}\right] \quad (1)$$

where Et_s is the scale parameter or the characteristic parameter, Et is the random variable (the measuring values of the cumulative breakdown strength), and $F(Et)$ indicates the cumulative failure probability for the Weibull distribution. The scale parameter, Et_s, represents the cumulative dielectric breakdown strength required for 63.2% of the tested specimens to fail. The

Table I. Weibull Parameters of Dielectric Strength of Each Samples

	Weibull parameter	
Samples	Shape (β)	Scale, Et_s (kV/mm)
Unfilled	65.85	53.44
2 vol % Al_2O_3	34.33	54.87
4 vol % Al_2O_3	52.85	45.04
6 vol % Al_2O_3	12.84	18.15
8 vol % Al_2O_3	45.39	8.48
2 vol % TiO_2	44.07	55.03
4 vol % TiO_2	54.57	51.99
6 vol % TiO_2	43.82	49.44
8 vol % TiO_2	46.12	46.76
2 vol % Organoclay	37.32	56.29
4 vol % Organoclay	33.23	52.47
6 vol % Organoclay	21.01	48.66
8 vol % Organoclay	26.81	46.36

shape parameter, β, a dimensionless number, is a measure of scattered values of the cumulative breakdown strength for $Et = Et_s$ and determines the shape of the probability density function. Two Weibull parameters obtained from Weibull distribution plots for Al_2O_3, TiO_2, and organoclay are summarized in Table I.

The dielectric breakdown strength data obtained from different loadings of Al_2O_3, TiO_2, and organoclay in the PP/EPDM blends were compared with the behavior of unfilled PP/EPDM in Figure 1. From this figure, the addition of 2 vol % of Al_2O_3, TiO_2, and organoclay slightly increases the dielectric breakdown strength of the nanocomposite system by 1.03, 1.59, and 2.85 kV, respectively. The addition of 2 vol % organoclay resulted in the highest breakdown strength as compared with other systems. The addition of Al_2O_3, TiO_2, and organoclay by more than 2 vol % substantially decreased the breakdown strength of the PP/EPDM nanocomposite.

Data from Table I shows the dependence of Weibull shape parameter, β, of the samples with respect to filler loading. The β-value shows breakdown distribution and dielectric reliability of the blend system. It can be observed that addition of 2 vol % Al_2O_3, TiO_2, and organoclay has reduced the β-value. Further addition of organoclay in PP/EPDM nanocomposites reduces the β-value. However, such behavior does not observed in PP/EPDM/TiO_2 and PP/EPDM/Al_2O_3 nanocomposites where the β shows inconsistent trend with the addition of Al_2O_3 and TiO_2 loadings. It is reported by previous work that this behavior is probably due to the heterogeneous distribution of Al_2O_3 and TiO_2 and aggregation phenomena of oxide particles.[19]

The increase in breakdown strength in vol % PP/EPDM with 2 vol % nanofillers can be explained by the barrier effect of the nanofillers. The tree propagation time in the PP/EPDM nanocomposite might be increased, and the accelerating test results show that the dielectric breakdown strength increased. When the filler content was increased, however, the defects at the interface, voids, and cracks increased and dielectric breakdown strength decreased.[20] However, the breakdown voltage in 4, 6, and 8 vol % Al_2O_3-filled PP/EPDM nanocomposites decreased because the Al_2O_3 nanoparticles tend to agglomerate [Figure 2(b)], and these clusters function as electrical defects. The addition of 4, 6, and 8 vol % TiO_2 also substantially weakened the PP/EPDM/TiO_2 nanocomposite. This result is due to the high permittivity of TiO_2, which indicates highly polar materials that contain dipoles.[21] Accordingly, TiO_2 has a low breakdown strength, which is consistent with the energy band gap of insulating materials.[22] The relative enhancements of 2 vol % organoclay-filled PP/EPDM nanocomposites are comparable to those in previous reports,[23] which also show a similar trend. The addition of a small amount of organoclay results in a gradual increase in breakdown strength, which is consistent with the obstruction of localized breakdown events. Thus, a supplementary and tortuous path exists between and around the inorganic molecules to reach the electrode.[24] At a high organoclay loading, the probability for the composites to form bereft regions is high, and a significant fraction of mesoscopic voids are located in regions between adjacent coherently stacked layers [Figure 2(d)]. Hence, the particle is not longer under the barrier effect and only contribute negatively to the electrical stability of the material by increasing the number of possible tree propagation paths.[25] The presence of voids in the PP/EPDM/Al_2O_3 nanocomposites significantly reduced the breakdown strength.[26] This result is due to a combination of two factors, namely, (a) air (which exists at the voids) has a lower breakdown strength than polymers and (b) the presence of a void creates local electric field strength irregularities, and the lower permittivity of air intensifies the electric field at the solid/void interface. Consequently, breakdown preferentially occurs first at a solid/void interface, which consequently disrupts the polymer structure and increases the void size.[27]

Dielectric Properties

The dielectric constant refers to the capability of a material to store electric potential energy under the effect of an alternative electric field.[28] The influence of filler loading and the effect of filler type as a function of frequency on the dielectric constant (ε') and dielectric loss (ε'') of Al_2O_3, TiO_2, and organoclay PP/EPDM nanomposites at various sweep frequencies are shown in Figures 3 and 4, respectively. The dielectric constant for various loadings of Al_2O_3, TiO_2, and organoclay shows frequency-independent behavior within a wide range of frequencies. However, an anomaly is shown in 8 vol % Al_2O_3 where the dispersion of real part of complex permittivity is observed in the system, and the trend is observed in the loss part as well (Figure 4). On the basis of the comparison between 2 and 8 vol % Al_2O_3, TiO_2, and organoclay-filled PP/EPDM nanocomposites, the dielectric constant increased with increasing addition of nanofiller particles. The enhancement of dielectric constant values for 8 vol % Al_2O_3, TiO_2, and organoclay in PP/EPDM nanocomposties compared with unfilled PP/EPDM and 2 vol % nanofiller in their respective systems is probably due to the significant contribution of the interfacial polarization, which is determined by the increased number of charges (impurities and

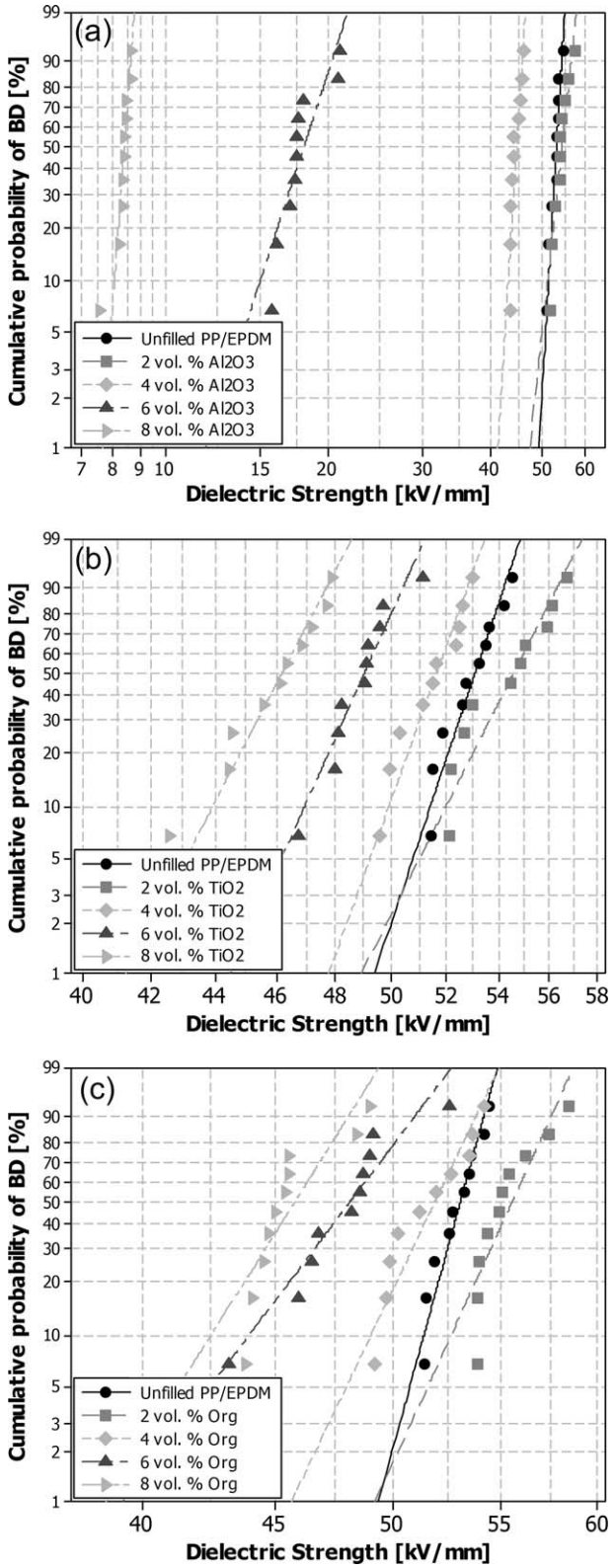

Figure 1. Weibull distribution plots for unfilled, 2, 4, 6, and 8 vol % (a) Al_2O_3, (b) TiO_2, and (c) Organoclay (Org) filled PP/EPDM nanocomposites.

small ions) introduced in the polymer by the nanoparticles.[29–31] PP/EPDM/TiO_2 had the highest dielectric constant, followed by PP/EPDM/Al_2O_3 and PP/EPDM/organoclay. The highest value of ε' was obtained from 8 vol % TiO_2-filled PP/EPDM nanocomposites because the TiO_2 used in the study consists of rutile phase, which has a high dielectric constant.[32]

The dielectric loss is a measure of the energy lost into a system during a cyclic electric excitation.[33] The value of dielectric loss is the highest for PP/EPDM/Al_2O_3, followed by PP/EPDM/TiO_2 and PP/EPDM/organoclay. The abrupt increase in dielectric loss of 8 vol % Al_2O_3 as compared to 2 vol % Al_2O_3 is clearly shown in Figure 4. As reported by previous work,[34] the dielectric loss is usually increased with increasing moisture content, polarization of water atoms, and free volume. Perhaps the absorbed moisture is hardly removed from Al_2O_3 as compared to other composite systems. A distinct increase in dielectric loss was also observed in the PP/EPDM/TiO_2 nanocomposites when the TiO_2 filler loading was increased. This result is in agreement with those of previous results and confirms the agglomeration of the filler and the enhancement in interfacial polarization at or about this volume percent.[30] The increase in dielectric loss in 2 and 8 vol % organoclay-filled PP/EPDM nanocomposites is also attributed to the entrapment of more charges in the PP/EPDM/organoclay nanocomposites, especially in the spacing between clay platelets. Thus, the conduction current is enhanced because of the inelastic displacements of charge carriers in the dielectric material.[34] It should be reiterated that the intercalation and exfoliation of organoclay might also govern the dielectric properties of polymeric nanocomposite materials.[35] In Figure 4, the frequency dependence of dielectric loss for the Al_2O_3, TiO_2, and organoclay-filled PP/EPDM nanocomposites is relatively stronger at higher frequencies than that of unfilled PP/EPDM blends. At higher frequencies, less time is required for charge migration to the interfaces and/or polarization of polymer chain dipoles. Thus, the dielectric loss decreases.[36] The negative dielectric loss observed at higher frequency is probably due to interference present in the measuring circuit. In addition, defects such as air gaps and the interfacial phase between the filler and the matrix in the composite materials can affect the dielectric constant and dielectric loss of the nanocomposites.[37] Therefore, a good insulation core would be a material with a low dielectric constant and a low dielectric loss at various frequencies.

Contact Angle Measurement

Contact angle measurement can be used to determine the hydrophobicity of the composite samples. Hydrophobicity is the ability of polymer nanocomposites to repel water on its surface, where individual droplets are formed rather than a film. This measurement is important in considering materials as outdoor insulators. The contact angle θ of a liquid droplet is defined as the angle formed between the tangent to the water droplet and the horizontal surface. In general, if the contact angle of the material is greater than 90°, then the material is hydrophobic. If the value is less than 90°, then the material is hydrophilic.[38] Figure 5 shows the dependence of contact angle of the samples with respect to filler loading. The contact angle of PP/EPDM/Al_2O_3 nanocomposites had an ascending trend with respect the increase in filler loading. On the other hand, the addition of TiO_2 and organoclay into the PP/EPDM blends gradually decreased the contact angle of the nanocomposites with respect

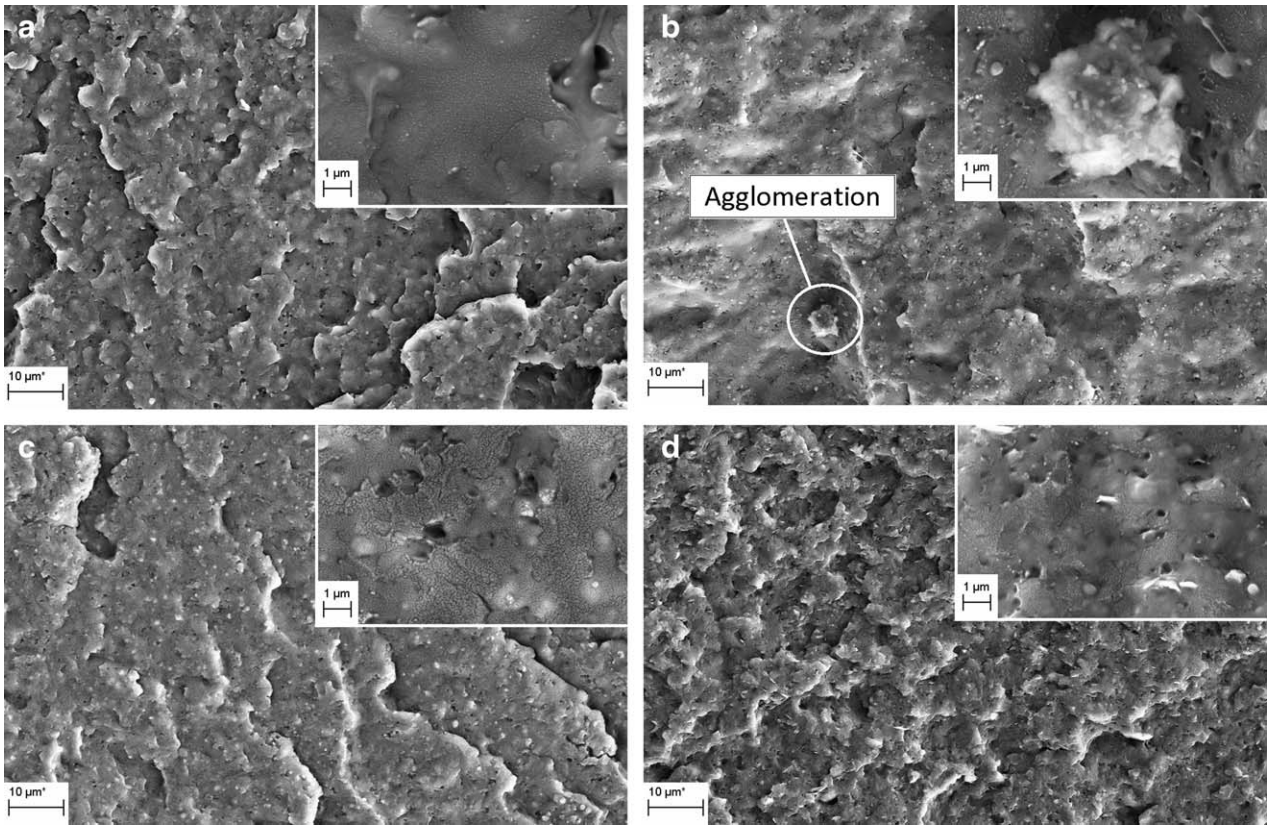

Figure 2. SEM micrograph showing fracture surface morphology of (a) unfilled, (b) 2 vol % Al_2O_3, (c) 2 vol % TiO_2, and (d) 2 vol %. Organoclay filled PP/EPDM nanocomposites (at ×1000 magnification). Insert figure refers to ×5000 magnification.

to filler loading, and the trend varies almost linearly. In general the contact angle of the composites is also governed by the contact angle of the nanofillers.

Previous studies conducted by Tadanaga et al.[39] and Karapanagiotis et al.[40] also observed the same trend of increasing hydrophobicity when the Al_2O_3 loading was increased. On the contrary, the increase in hydrophilicity of PP/EPDM/TiO_2 can be related to the hydroxyl groups that were formed on the surface of the PP/EPDM/ TiO_2 nanocomposites. The hydroxyl groups that were formed because of the presence of TiO_2 nanoparticles are polar. These polar groups can interact with water molecules through van der Waals' force and hydrogen bonds[41]; thus, the contact angle of the PP/EPDM/TiO_2 nanocomposites decreased. For the PP/EPDM/organoclay nanocomposite systems, the hydrophilicity had an increasing trend, which is in agreement with the results obtained by a previous study.[42] This trend is related to the hydrophilic nature of the clay

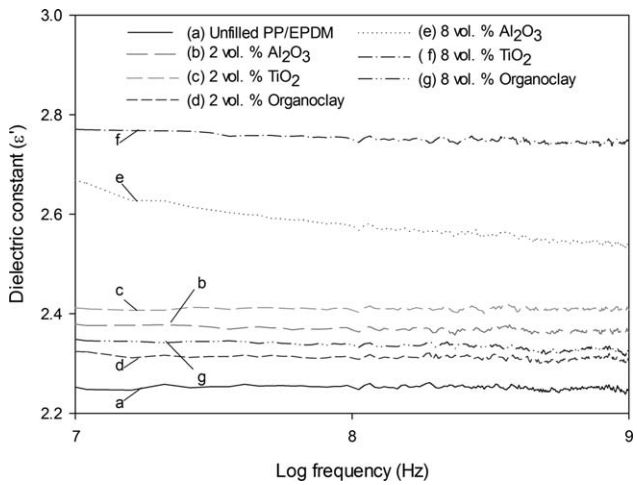

Figure 3. Behavior of dielectric constant (ε') of Al_2O_3, TiO_2, and organoclay filled PP/EPDM nanocomposites as a function of frequency.

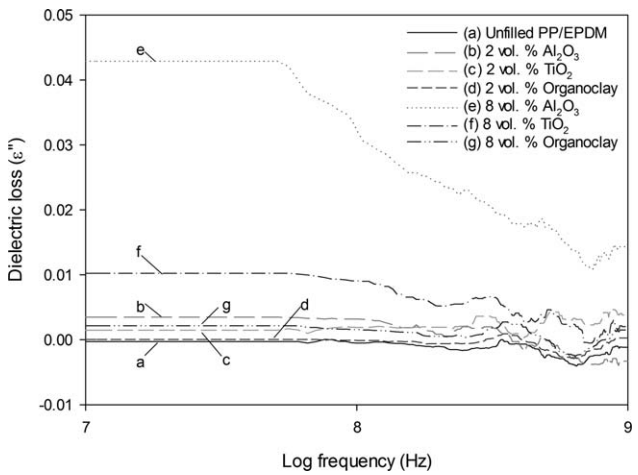

Figure 4. Behavior of dielectric loss (ε'') of Al_2O_3, TiO_2, and organoclay filled PP/EPDM nanocomposites as a function of frequency.

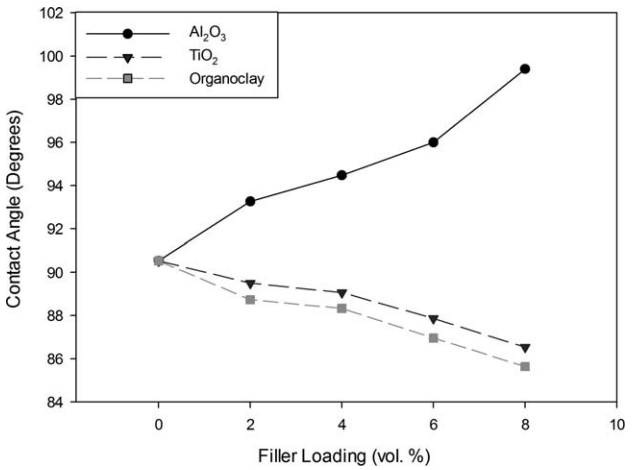

Figure 5. Variations in contact angle of Al_2O_3, TiO_2, and organoclay filled PP/EPDM nanocomposites.

incorporated, which results in the increase in surface hydrophilicity of the PP/EPDM/organoclay nanocomposites.[43]

Linear Rate of Burning

Polymers are known for their relatively high flammability. The tendency of polymers to spread flame away from a fire source is critical because many polymer melt and tend to produce flammable drips or flows.[44] Therefore, the horizontal burning test was performed to evaluate the rate of burning of PP/EPDM composite with the addition of Al_2O_3, TiO_2, and organoclay nanofillers, as depicted in Figure 6. The addition of Al_2O_3, TiO_2, and organoclay nanofillers has significant effects on the flammability of the PP/EPDM nanocomposites. These results show that the burning rate decreases after the addition of Al_2O_3, TiO_2, and organoclay as compared with that of the unfilled PP/EPDM composites, which had a rate of burning of 15.17 mm/min and had melting and dripping characteristics.

On the basis of Figure 6, at all filler loadings, the PP/EPDM/TiO_2 nanocomposites had the lowest linear burning rate, *V*, whereas the PP/EPDM/organoclay nanocomposites had the highest value. At a filler loading of 8 vol %, Al_2O_3, TiO_2, and organoclay had the lowest V-values in their systems, which are 10.51, 10.14, and 12.39 mm/min, respectively. The increase in Al_2O_3, TiO_2, and organoclay loadings increases the flame retardancy of the PP/EPDM composites. This result is strongly supported by the decrease in the burning rates of all three PP/EPDM composites.

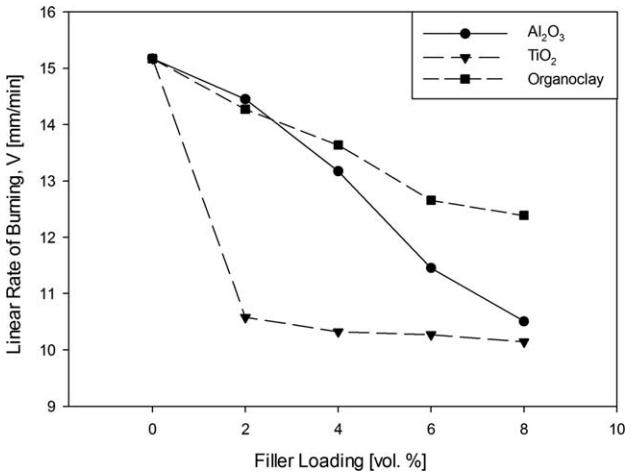

Figure 6. Effect of filler loading on linear burning rate of Al_2O_3, TiO_2, and organoclay filled PP/EPDM nanocomposites.

The addition of Al_2O_3 and TiO_2 in the PP/EPDM system reduces the ability of the nanocomposites to ignite and also reduces the heat release rate (HRR) peak. These results show a correlation with those of previous studies, where the addition of 15 vol % Al_2O_3 and TiO_2 into poly(methyl methacrylate) (PMMA) causes a reduction in the HRR peak by 274 and 277 kW m^{-2}, respectively, compared with that of virgin PMMA.[45] The reduction in the burning rate of the PP/EPDM/organoclay nanocomposites is due to the formation of a protective layer during combustion. This is in agreement with previous work where it is reported that organoclay is layered structure nanofillers, clay stacks and clay platelets that exist in the system have a possibility to reduce the burning rate of the polymer composite.[14,46] Upon heating, the viscosity of the molten polymer/layered silicate nanocomposite decreases with increasing temperature and facilitates the migration of clay nanolayers to the surface. Therefore, the accumulated clay on the surface of the material functions as a protective barrier that limits heat transfer into the material.[46]

CONCLUSIONS

The dielectric breakdown voltage shows that the addition of 2 vol % Al_2O_3, TiO_2, and organoclay into PP/EPDM blends increases the breakdown voltage of the PP/EPDM composites as compared with unfilled PP/EPDM. Further increasing the loadings of Al_2O_3, TiO_2, and organoclay until 8 vol % reduces the breakdown voltage of the composite. In terms of dielectric constant, the PP/EPDM/TiO_2 system exhibited the highest values, followed by PP/EPDM/Al_2O_3 and PP/EPDM/organoclay. The PP/EPDM/Al_2O_3 exhibited the highest dielectric loss as compared with PP/EPDM/TiO_2 and PP/EPDM/organoclay systems. The PP/EPDM/Al_2O_3 system shows an ascending trend of hydrophobicity, whereas an opposite trend was observed in PP/EPDM/TiO_2 and PP/EPDM/organoclay systems. The PP/EPDM/Al_2O_3 nanocomposites exhibited the lowest burning rate as compared with PP/EPDM/TiO_2 and PP/EPDM/organoclay systems. The nanocomposite filled with TiO_2 has better flame retardancy properties compared with those filled with Al_2O_3 and organoclay. In short, 2 vol % organoclay-filled PP/EPDM nanocomposites, which exhibit the highest dielectric breakdown strength, low dielectric constant, low dielectric loss, acceptable contact angle, and burning rate is suitable to be used as polymeric insulators.

ACKNOWLEDGMENTS

The authors gratefully acknowledge the Ministry of Higher Education of Malaysia for the Exploratory Research Grant Scheme (Grant number: 6730016). The authors would also like to acknowledge Universiti Sains Malaysia for the RU-PRGS grant (Grant number: 8036008).

REFERENCES

1. Li, Z.; Okamoto, K.; Ohki, Y.; Tanaka, T. *IEEE Trans. Dielectr. Electr. Insul.* **2010**, *17*, 653.
2. Danikas, M. G.; Tanaka, T. *IEEE Electr. Insul. M.* **2009**, *25*, 19.
3. Hackaml, R. *IEEE Trans. Dielectr. Electr. Insul.* **1999**, *6*, 557.
4. Ehsani, M.; Borsi, H.; Gockenbach, E.; Morshedian, J.; Bakhshandeh, G. R. *Eur. Polym. J.* **2004**, *40*, 2495.
5. Halimatuddahliana, I. H.; Akil, H. M. *Polym. Plast. Technol.* **2005**, *44*, 1429.
6. Khalili, S. M. R.; Farsani, R. E.; Rafiezadeh, S. *J. Reinf. Plast. Comp.* **2011**, *30*, 1341.
7. Arroyo, M.; Zitzumbo, R.; Avalos, F. *Polymer* **2000**, *41*, 6351.
8. Öksüz, M.; Eroglu, M.; Yildinm H. *J. Appl. Polym. Sci.* **2006**, *101*, 3033.
9. Yang, H.; Li, B.; Wang, K.; Sun, T.; Wang, X.; Zhang, Q.; Fu, Q.; Dong, X.; Han, C. C.; *Eur. Polym. J.* **2008**, *44*, 113.
10. Brostow, W.; Datashvili, T.; Hackenberg, K. P. *Polym. Compos.* **2010**, *31*, 1678.
11. Alipour, A.; Naderi, G.; Ghoreishy, M. H. *J. Appl. Polym. Sci.* **2013**, *127*, 1275.
12. Zarei, M.; Naderi, G.; Bakhshandeh, G. R.; Shokoohi, S. *J. Appl. Polym. Sci.* **2013**, *127*, 2038.
13. As'habi, L.; Jafari, S. H.; Khonakdar, H. A.; Kretzschmar, B.; Wagenknecht, U.; Heinrich, G. *J. Appl. Polym. Sci.* **2013**, *130*, 749.
14. Yildiz, D. E.; Apaydin, D. H.; Toppare, L.; Cirpan, A. *J. Appl. Polym. Sci.* **2013**, *128*, 1659.
15. Patra, A.; Bisoyi, D. K.; Manda, P. K.; Singh, A. K. *J. Appl. Polym. Sci.* **2013**, *128*, 1011.
16. Duan, J.; Shao, S.; Jiang, L.; Li, Y.; Jing, P.; Liu, B. *Iran. Polym. J.* **2011**, *20*, 855.
17. Hirose, H. *Electr. Eng. Jpn.* **1990**, *110*, 42.
18. Culver, S. P.; Beier, C. W.; Rafson, J. P.; Brutchey, R. L. *J. Appl. Polym. Sci.* **2014**, *131*, 4.
19. Laachachi, A.; Cochez, M.; Leroy, E.; Gaudon, P.; Ferriol, M.; Lopez Cuesta, J. M. *Polym. Adv. Technol.* **2006**, *17*, 327.
20. Cho, Y. S.; Shim, M. J.; Kim, S. W. *Compos. Interface* **2001**, *8*, 37.
21. Tan, D. Q.; Chen, Q.; Irwin, P.; Wang, Y. U. *Proc. ISAF-ECAPD-PFM* **2012**, 1.
22. Tan, D. Q.; Cao, Y.; Irwin, P. C. *Proc. Int. Confer. Solid Dielectr. ICSD* **2007**, 411.
23. Imai, T.; Sawa, F.; Nakano, T.; Ozaki, T.; Shimizu, T.; Kozako, M.; Tanaka, T. *IEEE Trans. Dielectr. Electr. Insul.* **2006**, *13*, 319.
24. Fillery, S. P.; Koerner, H.; Drummy, L.; Dunkerley, E.; Durstock, M. F.; Schmidt, D. F.; Vaia, R. A. *ACS Appl. Mater. Inter.* **2012**, *4*, 1388.
25. Tiemblo, P.; Hoyos, M.; Gómez-Elvira, J. M.; Guzmán, J.; García, N.; Dardano, A.; Guastavino, F. *J. Phys. D: Appl. Phys.* **2008**, *41*, 125208.
26. Huang, X.; Ma, Z.; Wang, Y.; Jiang, P.; Yin, Y.; Li, Z. *J. Appl. Polym. Sci.* **2009**, *113*, 3577.
27. Babrauskas, V. *Fire Mater.* **2006**, *30*, 151.
28. Chand, N.; Nigrawal, A. *J. Compos. Mater.* **2009**, *43*, 2859.
29. Panaitescu, D.; Ciuprina, F.; Iorga, M.; Frone, A.; Radovici, C.; Ghiurea, M.; Sever, S.; Plesa, I. *J. Appl. Polym. Sci.* **2011**, *122*, 1921.
30. Kashani, M. R.; Javadi, S.; Gharavi, N. *Smart Mater. Struct.* **2010**, *19*, 035019.
31. Kuang, X.; Gao, Q.; Zhu, H. *J. Appl. Polym. Sci.* **2013**, *129*, 296.
32. Minghua, C.; Jinghua, Y.; Yu, F.; Xiaoxu, L.; Guang L. Proceedings of the 6th International Forum on Strategic Technology, Institute of Electrical and Electronics Engineers (IEEE), Harbin, Heilongjiang, China, 2011, 155–158.
33. Su, J.; Chen, S.; Zhang, J.; Xu, Z. *J. Reinf. Plast. Compos.* **2010**, *29*, 2946.
34. Zilg, C.; Kaempfer, D.; Thomann, R.; Muelhaupt, R.; Montanari, G. C. Annual Reports on Electric Insulation and Dielectric Phenomena, Institute of Electrical and Electronics Engineers (IEEE), Albuquerque, NM, USA 2003, 546–550.
35. Mujumdar, A. S. Handbook of Industrial Drying, Chapter *12*; CRC Press: Boca Raton, FL, **2006**.
36. Tareev, B. Physics of Dielectric Materials, Chapter *2*; Mir Publishers: Moscow, **1975**, p 105.
37. Xiang, F.; Wang, H.; Yao, X. *J. Eur. Ceram. Soc.* **2007**, *27*, 3093.
38. Ehsani, M.; Bakhshandeh, G. R.; Morshedian, J.; Borsi, H.; Gockenbach, E. Proceeding of the 20th International Power System Conference, Iran Danesh Publication, Tehran, Iran, 2005, pp 1–8.
39. Tadanaga, K.; Katata, N.; Minami, T. *J. Eur. Ceram. Soc.* **1997**, *80*, 3213.
40. Karapanagiotis, I.; Manoudis, P. N.; Savva, A.; Panayiotou, C. *Surf. Interface Anal.* **2012**, *44*, 870.
41. Pourjafar, S.; Rahimpour, A.; Jahanshahi, M. *J. Ind. Eng. Chem.* **2012**, *18*, 1398.
42. Anadão, P.; Sato, L. F.; Wiebeck, H.; Valenzuela-Díaz, F. R. *Appl. Clay Sci.* **2010**, *48*, 127.
43. Corrales, T.; Larraza, I.; Catalina, F.; Portolés, T.; Ramírez-Santillán, C.; Matesanz, M.; Abrusci, C. *Biomacromolecules* **2012**, *13*, 4247.
44. Hamzah, M. S.; Mariatti, M. *J. Thermoplast. Compos. Mater.* **2013**, *26*, 1223.
45. Laachachi, A.; Cochez, M.; Leroy E.; Gaudon, P.; Ferriol, M.; Lopez-Cuesta, J. M. *Polym. Adv. Technol.* **2006**, *17*, 327.
46. Laoutid, F.; Bonnaud, L.; Alexandre, M.; Lopez-Cuesta, J. M.; Dubois, P. *Mater. Sci. Eng. R* **2009**, *63*, 100.